Received: 1 April 2021 | Revised: 6 June 2021 | Accepted: 26 June 2021

DOI: 10.1111/jace.18000

Journal of the American Ceramic Society

ORIGINAL ARTICLE

Effect of H_2 addition during PECVD on the moisture barrier property and environmental stability of H:SiN_x film

Jingyu Kim | Wooseok Jeong | Seunghee Lee | Sehun Jeong | Sang-Hee Ko Park

Department of Materials Science and Engineering, Korea Advanced Institute of Science and Technology (KAIST), Daejeon, Republic of Korea

Correspondence
Sang-Hee Ko Park, Department of Materials Science and Engineering, Korea Advanced Institute of Science and Technology (KAIST), 291 Daehak-ro, Yuseong-gu, Daejeon 34141, Republic of Korea.
Email: shkp@kaist.ac.kr

Funding information
National Research Foundation of Korea, Grant/Award Number: 2016R1A5A1009926 and 2018R1A2A3075518

Abstract

A hydrogenated silicon nitride (H:SiN_x) film with enhanced moisture barrier property and environmental stability was developed using plasma-enhanced chemical vapor deposition (PECVD) with the addition of H_2 gas at 100°C. The moisture barrier property and film density of the 100-nm-thick H:SiN_x film were ameliorated by increasing the H_2 gas flow rate during PECVD. X-ray photoelectron spectroscopy and Fourier-transform infrared spectroscopy studies demonstrated that the improved performance was a result of an increase in the amount of Si–N bonds compared to hydrogen-terminated bonds with an increase in the H_2 gas flow rate. It is believed that H_2 gas assisted the formation of aminosilane, which contributed to the condensation of silicon nitride by lowering the activation energy for radicalization reactions of silane and ammonia. After the 85°C/85% RH test, the optimized H:SiN_x film maintained a water vapor transmission rate lower than 5×10^{-5} g/m^2/day owing to the suppression of oxidation. The optimized H:SiN_x film was rarely oxidized owing to the decrease in hydrogen-terminated bonds and increase in the film density. The results indicated that the introduction of H_2 gas during the PECVD process strengthened the environmental stability of the H:SiN_x film.

KEYWORDS

environmental stability, H:SiN_x, H_2 gas, moisture barrier property, PECVD

1 | INTRODUCTION

Flexible electronic devices, which are gaining immense popularity in the market, are continuously being developed for advanced performance. In particular, organic light-emitting diodes (OLEDs), which are major components of flexible and foldable displays, have been widely researched because they have excellent self-lighting characteristics and do not require a rigid backlight unit.[1,2] However, the deterioration of emission characteristics due to moisture attack necessitates thin film passivation of OLEDs to improve their durability. Moreover, thin films deposited at low temperatures generally do not provide sufficient moisture barrier properties.[3–6] Therefore, achieving thin-film passivation along with excellent moisture barrier properties using low-temperature processes has become one of the most important and challenging activities.

The thin-film passivation architecture consists mainly of a multi-dyad structure composed of alternating inorganic and organic layers. Multi-dyad structures can minimize pinhole propagation in the inorganic layer and elongate the effective path of water vapor by means of the lag time effect.[7–10] Various inorganic materials such as Al_2O_3, TiO_2, and SiN_X have been used in multi-dyad structures, and they all exhibit excellent moisture barrier properties.[11–13] In a multi-dyad structure, the water vapor transmission rate (WVTR) decreases as the number of stacks increases. Nevertheless, the increased number of stacks not only makes the process complex but also limits flexibility by increasing the overall thickness. From this point of view, it is essential to decrease

the number of stacks while maximizing the moisture barrier property of the passivation film.

In addition to the minimization of water vapor permeability, enhancement of the environmental stability of thin-film passivation is also important.[11,14,15] In general, when an inorganic thin film deposited at low temperature is exposed to moisture for a long time at elevated temperatures, the moisture barrier property of the thin film passivation is degraded. It has been reported that the introduction of a protective layer in the thin film passivation can suppress the degradation of the inorganic layer by moisture attack.[11] However, in this case, additional processes are required to deposit the protective layer. Therefore, it is necessary to develop an inorganic layer with high stability under high moisture and temperature conditions.

Herein, we report the enhanced moisture barrier property and environmental stability of a single H:SiN_x film deposited by plasma-enhanced chemical vapor deposition (PECVD) at 100°C through the addition of H_2 gas. The water vapor permeability of the H:SiN_x film was minimized to less than 5×10^{-5} g/m^2/day by controlling the flow rate of H_2 gas during PECVD. In addition, the effects of H_2 gas introduction on the chemical properties of the H:SiN_x film and the relationship between the chemical properties and the water vapor permeability were investigated. To ascertain the environmental stability of the H:SiN_x film, the water vapor permeability and the chemical properties of the H:SiN_x films were investigated after an 85°C/85% relative humidity (RH) test (8585 test).

2 | EXPERIMENTAL PROCEDURE

2.1 | Sample preparation

A 75-μm-thick polyethylene terephthalate (PET; DAVO C&M) film was used as a substrate for the deposition of H:SiN_x film for measuring WVTR. In other analyzes except for WVTR measurement, Si wafer was used as the substrate. The PET film was initially sonicated in an isopropyl alcohol bath followed by a deionized water bath for 15 min to remove surface contaminants. A 100-nm-thick H:SiN_x film was deposited by PECVD with a chamber size of 200 mm × 200 mm at 100°C. The flow rates of silane (SiH_4) and ammonia (NH_3) were fixed at 30 and 120 sccm, respectively. To investigate the effect of H_2 gas on the properties of H:SiN_x films, the films were deposited at H_2 gas flow rates of 300 (HSN300), 700 (HSN700), and 1000 sccm (HSN1000), respectively. In addition, an H:SiN_x film was fabricated using Ar gas at a flow rate of 1000 sccm (ASN1000) for comparison with the H:SiN_x film deposited using H_2 gas. The deposition conditions of the H:SiN_x films are listed in Table 1.

2.2 | Characterization

The thickness and the refractive index of the H:SiN_x films were determined using an ellipsometer (ALPHA-SE, J.A. Woollam). The WVTR of the H:SiN_x film was measured using Aquatran 2 (MOCON), which has a measurement limit of 5×10^{-5} g/m^2/day. The area exposed to water vapor was 50 cm^2, and the WVTR measurement conditions were 100% RH at 38°C. The WVTR measurements were recorded every 8 h for 3 days. To analyze the environmental stability of the H:SiN_x films, samples were conducted for 7 days in a chamber maintained at 85°C/85% RH and WVTR was measured for comparison before and after 8585 test.

X-ray reflectivity (XRR) analysis was performed using a high-resolution X-ray diffractometer (SmartLab, Rigaku) to determine the density of the H:SiN_x film based on the critical angle of the calculated curve. The structure model was a four-layer system comprising a Si wafer substrate, native silicon oxide, hydrogenated silicon nitride, and surface silicon oxide. To obtain the etch rate of the H:SiN_x films, wet etching was carried out with a diluted hydrogen fluoride (HF) etchant at 25°C. The etchant was prepared by mixing water and HF in a volume ratio of 300:2. The etch rates of the H:SiN_x films were determined by measuring the difference in thickness obtained by ellipsometry before and after wet etching.

X-ray photoelectron spectroscopy (XPS; K-alpha, Thermo VG Scientific) with an Al K-alpha X-ray source was used to analyze the chemical composition of the H:SiN_x films. Presputtering with Ar ions (3 keV) was performed for 120 s to remove contaminants on the surface of the H:SiN_x films. All the scanned spectra were charge-shifted based on the Ar 2*p* peak at 241.9 eV.

Fourier-transform infrared spectroscopy (FTIR) of the H:SiN_x films was carried out using a Nicolet iS50 (Thermo

TABLE 1 PECVD process conditions of H:SiN_x films

	Temperature (°C)	Power (W)	Working pressure (Torr)	Gas ratio (sccm)
HSN300	100	100	1.5	SiH_4:NH_3:H_2 = 30:120:300
HSN700	100	100	1.5	SiH_4:NH_3:H_2 = 30:120:700
HSN1000	100	100	1.5	SiH_4:NH_3:H_2 = 30:120:1000
ASN1000	100	100	1.5	SiH_4:NH_3:Ar = 30:120:1000

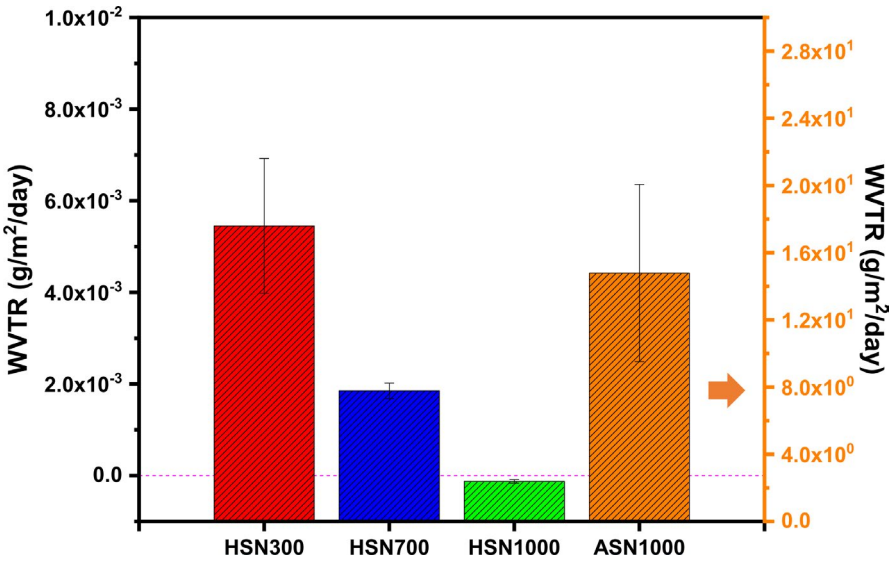

FIGURE 1 The WVTR average values of HSN300, HSN700, HSN1000, and ASN1000

Fisher Scientific Instrument) spectrometer in transmission mode. All the FTIR spectra were subjected to baseline correction to compare the intensities of the vibration modes of each H:SiN$_x$ film.

The surface oxidation of the H:SiN$_x$ films was studied using an atomic force microscope (AFM; XE-100, Park Systems). The AFM images were obtained over an area of 3 μm × 3 μm, and the roughness was calculated using the root mean square method. Transmission electron microscopy (TEM; Libra 200 HT Mc, Carl Zeiss) and energy dispersive spectroscopy (EDS) were used to visually illustrate the degree of oxidation in the H:SiN$_x$ samples.

3 | RESULTS AND DISCUSSION

3.1 | Moisture barrier properties of H:SiN$_x$ films

The moisture barrier properties of the H:SiN$_x$ films deposited under different gas conditions were studied by measuring the WVTR of the H:SiN$_x$ films using a MOCON permeation analyzer. The WVTR values of HSN300, HSN700, HSN1000, and ASN1000 are averaged over four samples, shown in Figure 1. After 72 h of MOCON testing, the WVTRs of HSN300, HSN700, and HSN1000 were 5.452×10^{-3}, 1.853×10^{-3}, and -1.230×10^{-4} g/m^2/day, respectively. Aquatran 2 has a measurement limit of 5×10^{-5} g/m^2/day, and the negative value of WVTR indicates that it is lower than 5×10^{-5} g/m^2/day. Therefore, the WVTR of HSN1000 is lower than 5×10^{-5} g/m^2/day. As shown in Figure 1, the moisture barrier property of the H:SiN$_x$ film improved considerably with an increase in the H_2 gas flow rate during PECVD. Meanwhile, the WVTR of ASN1000 was 1.478×10^{1} g/m^2/day under the same conditions, indicating that Ar gas could not reinforce the moisture barrier property of the H:SiN$_x$ film. From the WVTR results of the H:SiN$_x$ films, it can be inferred that introducing H_2 gas enhances the moisture barrier properties.

TABLE 2 Elemental composition and refractive index of H:SiN$_x$ films obtained from the XPS profiles

	Si (at.%)	N (at.%)	O (at.%)	n
HSN300	55.02	42.05	2.930	1.814
HSN700	53.69	44.33	1.980	1.853
HSN1000	53.30	44.60	2.100	1.860
ASN1000	50.46	45.63	3.910	1.741

3.2 | Characterization of the barrier properties of the H:SiN$_x$ films

The chemical compositions and the refractive indices of HSN300, HSN700, HSN1000, and ASN1000 were obtained from XPS and ellipsometry analyses, respectively, and are listed in Table 2. According to the XPS analysis, all the H:SiN$_x$ films contained less than 4 at% oxygen. Oxygen is slightly contained in the composition of H:SiN$_x$ films due to small amounts of oxygen species in the PECVD chamber or leakage of the N_2O gas line. This suggests that the bulk of the H:SiN$_x$ films was fully silicon nitride with a little amount of oxygen. The refractive index values of the samples also confirm that all the films were composed of silicon nitride.[16] With an increase in the H_2 gas flow rate during PECVD, the refractive index tended to increase slightly. The change in the refractive index is likely due to the difference in the film density or chemical bonding structure.[17]

According to the XRR analysis, the densities of HSN300, HSN700, HSN1000, and ASN1000 films were 2.07, 2.11, 2.21, and 1.93 g/cm^3, respectively, as shown in Figure 2.

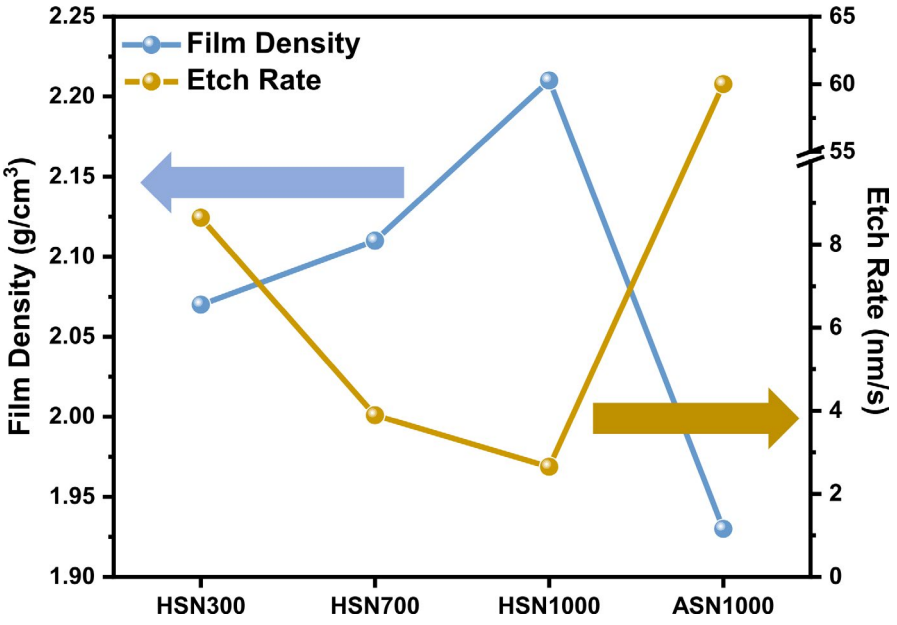

FIGURE 2 Film density and etch rate of HSN300, HSN700, HSN1000, and ASN1000. The film density and the etch rate were determined by XRR and diluted HF etching test, respectively

While the film density of the H:SiN$_x$ increased with an increase in the H_2 gas flow, the addition of Ar gas yielded a rather porous film. The film density is known to be inversely proportional to WVTR because it is difficult for water molecules to pass through a dense film.[18] Wet etching tests were carried out on each H:SiN$_x$ film to confirm the trend of the film density results. Figure 2 shows that the etch rates of HSN300, HSN700, HSN1000, and ASN1000 are 8.641, 3.891, 2.650, and 60.00 nm/s, respectively. As the film density of silicon nitride increases, the etch rate of silicon nitride generally decreases since it is difficult for the etchants to penetrate the film.[19] Therefore, the etch rates of the H:SiN$_x$ films correspond to the relationship between the film density and the etch rate of silicon nitride. In the case of ASN1000, the etch rate was much higher than that of other H:SiN$_x$ films. Thus, the XRR analysis and the wet etching results show that Ar gas is not effective for the densification of the H:SiN$_x$ film in PECVD. In contrast, H_2 gas was found to be beneficial for improving the film density of H:SiN$_x$. Further analyses of HSN300, HSN700, and HSN1000 films were conducted to determine the effect of H_2 gas flow rate during PECVD on the chemical bonding structure.

XPS analysis was performed to determine the difference in the chemical bonding states of the H:SiN$_x$ films. Figure 3A–C shows the deconvolution of the Si 2p XPS profiles of HSN300, HSN700, and HSN1000. The Si 2p peak of all the samples was deconvoluted into two subpeaks consisting of Si–H bond (~99.9 eV) and Si–N bond (~101.4 eV).[20,21] As shown in Figure 3D, the quantitative ratios of Si–H bond to Si–N bond in HSN300, HSN700, and HSN1000 are 0.26, 0.19, and 0.12, respectively. Compared to the Si–H bonds, the amount of Si–N bonds in the H:SiN$_x$ samples increased with an increase in the H_2 gas during the PECVD process.

FTIR analysis was conducted to determine the chemical bonding structure of the H:SiN$_x$ film. Figure 3E shows the FTIR spectra of HSN300, HSN700, HSN1000. All the spectra clearly show the presence of Si–N stretching mode (~835 cm^{-1}), N–H bending mode (~1174 cm^{-1}), Si–H stretching mode (~2160 cm^{-1}), and N–H stretching mode (~3360 cm^{-1}).[22] The normalized intensities of the vibration modes based on the absorbance in the FTIR spectra are shown in Figure 3F. As more H_2 gas was added during PECVD, the normalized intensity of the Si–N stretching mode increased. Conversely, the normalized intensity of the N–H bending mode, Si–H stretching mode, and N–H stretching mode decreased as the H_2 gas flow rate increased. Generally, Si–N bonds can induce the increase in film density of silicon nitride.[23] However, hydrogen-terminated bonds such as Si–H and N–H bonds do not significantly contribute to the increase in film density of silicon nitride.[23] As previously stated, it is known that the increase in film density is inversely proportional to the WVTR. Therefore, more Si–N bonds have an effect on increasing the film density and decreasing the WVTR.

The results of the XPS and the FTIR analyses are shown in Figure 3D,F, respectively. As the H_2 flow rate increased, the amount of Si–N bonds increased compared to the hydrogen-terminated bonds. In the case of PECVD using SiH_4 and NH_3, aminosilane is a known source of silicon nitride formation.[24] Reactions among the aminosilanes themselves on the surface create Si–N bonds, which condense the silicon nitride. Aminosilane is produced by the reaction between SiH_4 and NH_3 radicals.[25] Therefore, to increase the amount of aminosilane, the radicalization of SiH_4 and NH_3 should be promoted. When hydrogen gas was introduced in PECVD, the activation energy for the radical formation of SiH_4 and NH_3 was greatly decreased to accelerate the reaction.[26] Unlike Ar

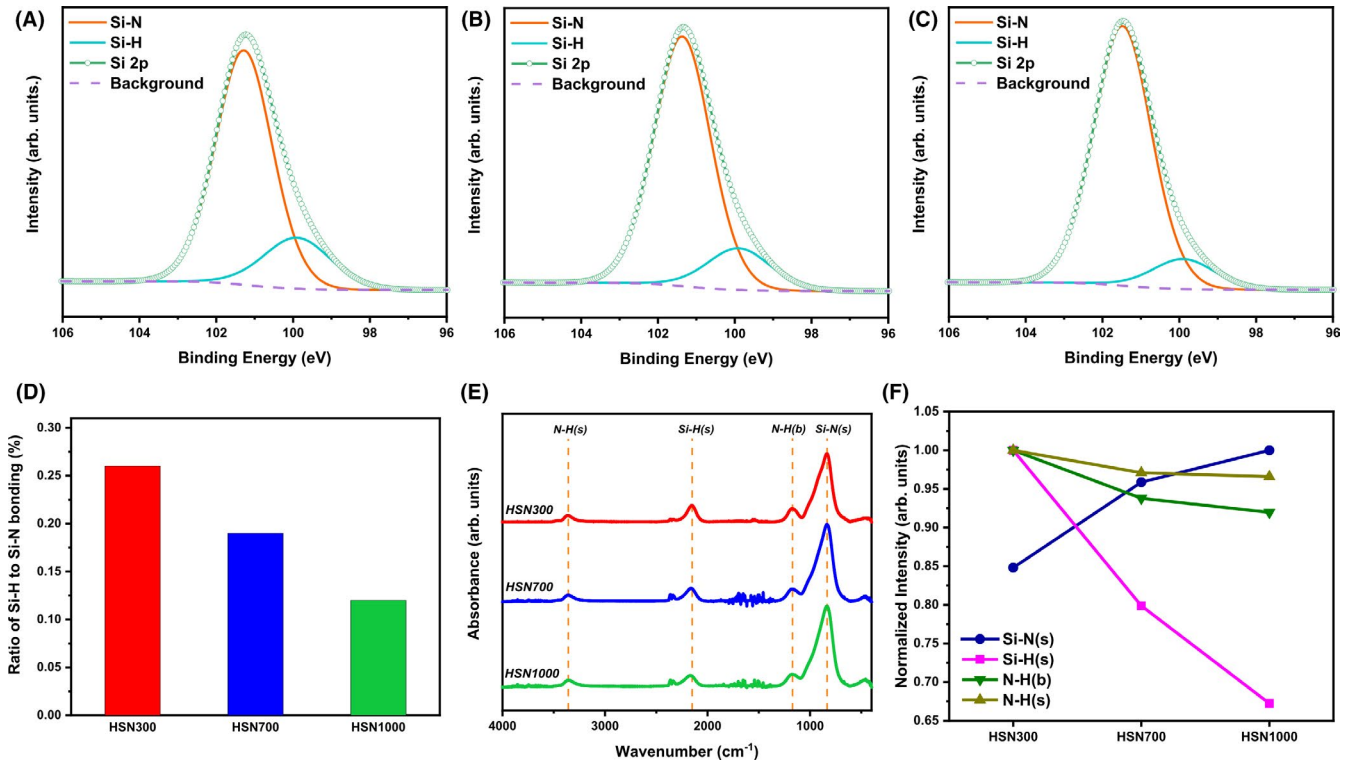

FIGURE 3 Deconvoluted Si 2p X-ray photoelectron peak obtained from the bulk region of (A) HSN300, (B) HSN700, (C) HSN1000, and (D) Quantitative ratio of Si–H bond to Si–N bond in HSN300, HSN700, and HSN1000. (E) FTIR absorbance spectra of HSN300, HSN700, and HSN1000. (F) Normalized intensity of vibration modes based on the FTIR absorbance spectra of HSN300, HSN700, and HSN1000

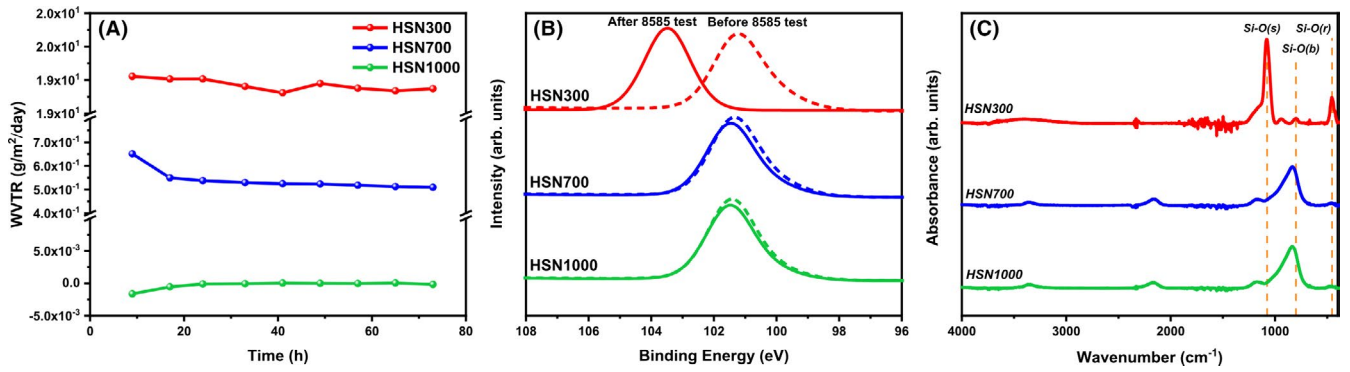

FIGURE 4 (A) WVTR values of HSN300, HSN700, and HSN1000 after the 8585 test. The WVTR was measured every 8 h for 72 h. (B) Si 2p X-ray photoelectron peak obtained from the bulk region of HSN300, HSN700, and HSN1000 before and after the 8585 test. (C) FTIR absorbance spectra of HSN300, HSN700, and HSN1000 after the 8585 test

gas, which is an inert gas, H_2 gas assists the radicalization of SiH_4 and NH_3. This increases the amount of Si–N bond, which enhances the film density of silicon nitride.

3.3 | Environmental stability of H:SiN_x films

The WVTRs of HSN300, HSN700, and HSN1000 after the 8585 test were used to analyze the environmental stability of the H:SiN_x films and the results are shown in Figure 4A. After 72 h of MOCON testing, the WVTRs of HSN300, HSN700, and HSN1000 were 1.887×10^{1}, 5.095×10^{-1}, and -1.843×10^{-1} g/m^2/day, respectively. Compared to the results in Figure 1A, the WVTRs of HSN300 and HSN700 increased considerably. In contrast, HSN1000 did not show any change in the WVTR after the 8585 test. This result demonstrates that HSN1000 has superior environmental stability compared to the other films.

The changes in the chemical properties of HSN300, HSN700, and HSN1000 were analyzed by XPS and FTIR. Figure 4B shows the Si 2p XPS profiles of HSN300, HSN700, and HSN1000 before (dotted curve) and after (solid curve) the 8585 test. In the case of HSN300, the position of the Si 2p peak shifted from 101.3 to 103.5 eV after the 8585 test. The binding energy of the Si–O bond subpeak (~103.3 eV) indicates that HSN300 was fully oxidized after the 8585 test.[27] In contrast, the positions of the Si 2p peaks of HSN700 and HSN1000 shifted slightly from 101.4 to 101.5 eV after the 8585 test. This result indicates that the bulk of HSN700 and HSN1000 was only slightly oxidized after the 8585 test. The FTIR spectra of HSN300, HSN700, and HSN1000 after the 8585 test are shown in Figure 4C. The FTIR profile of HSN300 exhibited the Si–O rocking mode (~460 cm^{-1}), Si–O bending mode (~800 cm^{-1}), Si–O stretching mode (~1080 cm^{-1}), and O–H stretching mode (~3410 cm^{-1}).[28] Compared with the FTIR results in Figure 3E, the Si–N and Si–H vibration modes disappeared, and Si–O and O–H vibration modes appeared, which indicates complete oxidization of HSN300. Meanwhile, the FTIR spectra of HSN700 and HSN1000 showed the same vibration modes observed before the 8585 test without any indication of the presence of Si–O and O–H vibration modes. This indicates that HSN700 and HSN1000 were hardly oxidized compared to HSN300. These results are consistent with the XPS results shown in Figure 4B.

Silicon nitride easily reacts with water molecules in a moist environment. This process forms thermodynamically stable Si–O bonds and O–H bonds in silicon nitride.[29] In particular, it is known that Si–H bond and N–H bond accelerate the oxidation process of silicon nitride.[15] As shown in Figure 3F, the normalized intensities of the vibration modes related to Si–H and N–H bonds are the largest in HSN300. Therefore, the presence of large amounts of Si–H and N–H bonds in HSN300 seemed to make the film vulnerable to oxidation. In addition, it is difficult for water molecules to penetrate the lattice of dense films during oxidation. A substantial amount of hydrogen-terminated bonds in HSN300 promoted the oxidation process of silicon nitride compared to the cases of HSN700 and HSN1000. It is known that the increase in the WVTR of silicon nitride originated from the change in the chemical bonding state to silicon oxide through oxidation.[30] Therefore, oxidation of the film increases the WVTRs of HSN300 and HSN700. However, no evidence of oxidation was found in the XPS and FTIR analyses of HSN700 despite the decrease in the WVTR after the 8585 test. Hence, it is believed that the oxidation did not proceed to the bulk of HSN700, but occurred only at the surface.

AFM studies were performed to analyze the surface oxidation of the H:SiN_x films before and after the 8585 test. The two-dimensional AFM images of HSN300, HSN700, and HSN1000 are shown in Figure 5. After the 8585 test, the roughness values of HSN300, HSN700, and HSN1000 changed from 0.55 to 1.65 nm, 0.28 to 0.51 nm, and 0.24 to 0.23 nm, respectively, as exhibited in Figure 5A,B. The roughness increased significantly in the cases of HSN300 and HSN700, and the changes in the topology are evident from the AFM images. However, no significant change was observed in the roughness and topology of HSN1000. These results suggest that HSN1000 has superior resistance to oxidation compared to HSN300 and HSN700.

To visually illustrate the degree of oxidation of the H:SiN_x films before and after the 8585 test, TEM studies of HSN300, HSN700, and HSN1000 were carried out. The TEM and TEM-EDS mapping images of HSN300, HSN700, and HSN1000 are shown in Figure 6A–C. After the 8585 test, the thickness of HSN300 was approximately 140 nm, which is 40 nm greater than the original thickness, because of volume expansion by oxidation. In addition, the TEM-EDS mapping image of HSN300 shows the presence of oxygen throughout the thickness of the coating. Thus, it can be considered that HSN300 was fully

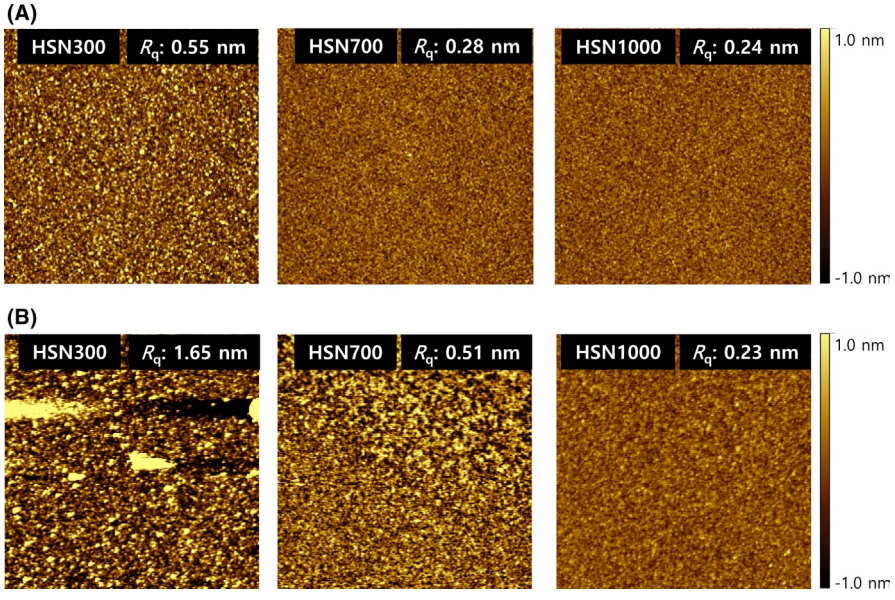

FIGURE 5 AFM images of HSN300, HSN700, and HSN1000 (A) before and (B) after the 8585 test

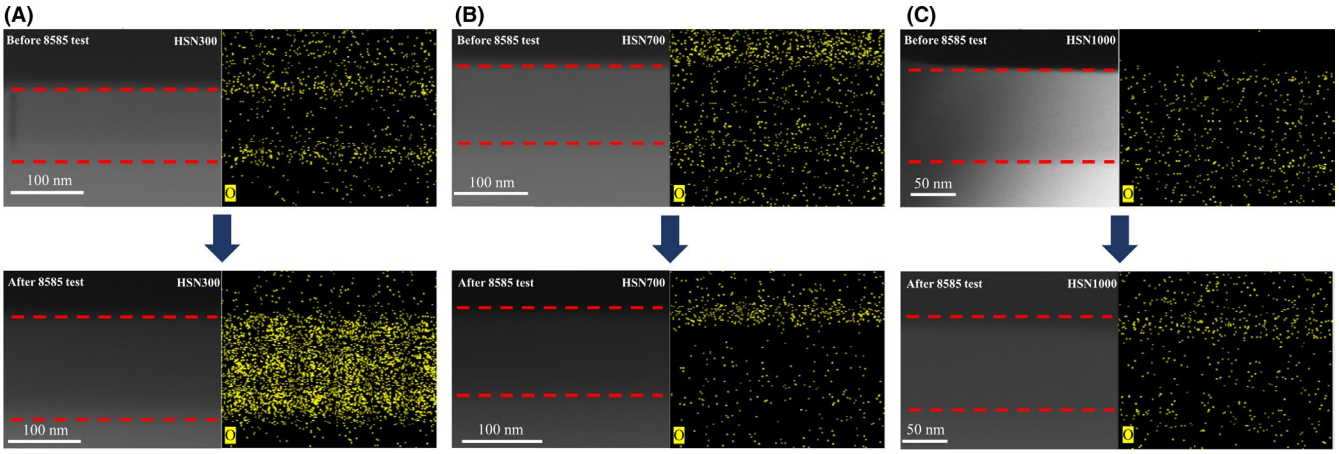

FIGURE 6 TEM images and TEM-EDS mapping images of (A) HSN300, (B) HSN700, and (C) HSN1000 before and after the 8585 test

oxidized after the 8585 test. On the contrary, the thicknesses of HSN700 and HSN1000 hardly changed after the 8585 test. In addition, little oxygen component is detected in the TEM-EDS mapping images of HSN700 and HSN1000 bulk regions, even after the 8585 test. However, more oxygen components are observed on the surface of the HSN700 compared to that of the HSN1000 after the 8585 test as shown in Figure 6B,C. These results suggest that more oxidation proceeded on the surface of HSN700 than HSN1000 after the 8585 test. Therefore, it was visually demonstrated that HSN1000 has outstanding environmental stability than other samples.

4 | CONCLUSIONS

A thin H:SiN_x passivation film with enhanced moisture barrier property and environmental stability was developed by H_2 gas addition in PECVD. The moisture barrier property and film density improved with an increase in the H_2 gas flow rate. Specifically, HSN1000 with a thickness of 100 nm showed outstanding moisture barrier property with values lower than 5×10^{-5} g/m^2/day. According to the XPS and FTIR analyses, the improvement in the film density can be attributed to an increase in the amount of Si–N bonds and a decrease in the amount of hydrogen-terminated bonds such as Si–H and N–H in silicon nitride. H_2 was considered to contribute to the formation of dense silicon nitride as a result of the formation of more aminosilanes by lowering the activation energy for the radicalization reactions of SiH_4 and NH_3. Unlike HSN300 and HSN700, the moisture barrier property of HSN1000 was maintained even after the 8585 test for 7 days. The degradation in the moisture barrier properties of HSN300 and HSN700 was due to oxidation during the 8585 test, as confirmed using XPS, FTIR, and AFM analyses. The TEM and TEM-EDS illustrated that HSN1000 is inert to the environment, resulting in improved moisture barrier properties.

ACKNOWLEDGMENTS

This work was supported by the Wearable Platform Materials Technology Center (WMC) funded by the National Research Foundation of Korea (NRF) Grant by the Korean Government (MSIP) (No. 2016R1A5A1009926) and the National Research Foundation of Korea (NRF) grant funded by the Korea government (MSIT) (No. 2018R1A2A3075518).

ORCID

Sang-Hee Ko Park https://orcid.org/0000-0001-7165-8211

REFERENCES

1. Salehi A, Fu X, Shin DH, So F. Recent advances in OLED optical design. Adv Funct Mater. 2019;29(15):1808803.
2. Jeon Y, Choi HR, Park KC, Choi KC. Flexible organic light-emitting-diode-based photonic skin for attachable phototherapeutics. J Soc Inf Disp. 2020;28(4):324–32.
3. Aziz H, Xu G. A degradation mechanism of organic light-emitting devices. Synth Met. 1996;80(1):7–10.
4. Schaer M, Nüesch F, Berner D, Leo W, Zuppiroli L. Water vapor and oxygen degradation mechanisms in organic light emitting diodes. Adv Funct Mater. 2001;11(2):116–21.
5. Lee JS, Sahu BB, Han JG. Effect of the RF power on the characteristic properties of high-performance silicon nitride single-layer permeation barriers. Surf Coat Technol. 2019;364:63–9.
6. Kim SJ, Yong SH, Ahn HJ, Shin Y, Chae H. Improvement in the moisture barrier properties and flexibility by reducing hydrogen dangling bonds in SiNx thin films with plasma surface treatment. Surf Coat Technol. 2020;383:125210.
7. Graff GL, Williford RE, Burrows PE. Mechanisms of vapor permeation through multilayer barrier films: Lag time versus equilibrium permeation. J Appl Phys. 2004;96(4):1840–9.
8. Kim N, Potscavage WJ, Sundaramoothi A, Henderson C, Kippelen B, Graham S. A correlation study between barrier film performance and shelf lifetime of encapsulated organic solar cells. Sol Energy Mater Sol Cells. 2012;101:140–6.
9. Kwon JH, Jeon Y, Choi S, Park JW, Kim H, Choi K. C, Functional design of highly robust and flexible thin-film encapsulation

composed of quasi-perfect sublayers for transparent, flexible displays. ACS Appl Mater Interfaces. 2017;9(50):43983–92.
10. Wu J, Fei F, Wei C, Chen X, Nie S, Zhang D, et al. Efficient multi-barrier thin film encapsulation of OLED using alternating Al_2O_3 and polymer layers. RSC Adv. 2018;8:5721–7.
11. Kwon JH, Jeong EG, Jeon Y, Kim DG, Lee S, Choi KC. Design of highly water resistant, impermeable, and flexible thin-film encapsulation based on inorganic/organic hybrid layers. ACS Appl Mater Interfaces. 2019;11(3):3251–61.
12. Han D-S, Choi D-K, Park J-W. Al_2O_3/TiO_2 multilayer thin films grown by plasma enhanced atomic layer deposition for organic light-emitting diode passivation. Thin Solid Films. 2014;552:155–8.
13. Kim N, Graham S. Development of highly flexible and ultra-low permeation rate thin-film barrier structure for organic electronics. Thin Solid Films. 2013;547:57–62.
14. Jeong EG, Han YC, Im H-G, Bae B-S, Choi KC. Highly reliable hybrid nano-stratified moisture barrier for encapsulating flexible OLEDs. Org Electron. 2016;33:150–5.
15. Oh MH, Park EK, Kim SM, Heo J, Kim HJ. Long-term stability of SiNx thin-film barriers deposited by low temperature PECVD for OLED. ECS J. Solid State Sci Technol. 2016;5(5):R55–8.
16. Gleskova H, Wagner S, Gašparık V, Kováč P. Low-temperature silicon nitride for thin-film electronics on polyimide foil substrates. Appl Surf Sci. 2001;175:12–6.
17. Lee J-W, Ryoo R, Jhon MS, Cho K-I. Bond density and physicochemical properties of a hydrogenated silicon nitride film. J Phys Chem Solids. 1995;56(2):293–9.
18. Zhang H, Ding H, Wei M, Li C, Wei B, Zhang J. Thin film encapsulation for organic light-emitting diodes using inorganic/organic hybrid layers by atomic layer deposition. Nanoscale Res Lett. 2015;10:169.
19. Claassen W, Valkenburg W, Wijgert W, Willemsen M. On the relation between deposition conditions and (mechanical) stress in plasma silicon nitride layers. Thin Solid Films. 1985;129(3–4):239–47.
20. Swain BP, Swain BS, Park SH, Hwang NM. Plasmon loss and valence band structure of silicon-based alloys deposited by hot wire chemical vapor deposition. J. Alloys Compd. 2009;480:878–81.
21. Xu X, Zhou D, He Q, Jiang J, Fan T, Huang L, et al. Chemical control of physical properties in silicon nitride films. Appl Phys A. 2013;111:867–76.
22. Kobayashi S-I. IR spectroscopic study of silicon nitride films grown at a low substrate temperature using very high frequency plasma-enhanced chemical vapor deposition. World J Condens Matter Phys. 2016;06(04):287–93.
23. Sato M, Takeyama MB, Nakata Y, Kobayashi Y, Nakamura T, Noya A. Low-temperature-deposited insulating films of silicon nitride by reactive sputtering and plasma-enhanced CVD: Comparison of characteristics. Jpn J Appl Phys. 2016;55(4S):04EC05.
24. Smith DL, Alimonda AS, Chen CC, Ready SE, Wacker B. Mechanism of SiN_xH_y deposition from NH_3-SiH_4 plasma. J Electrochem Soc. 1990;137(2):614.
25. Beach D, Jasinski J. Excimer laser photochemistry of silane-ammonia mixtures at 193 nm. J Phys Chem. 1990;94(7):3019–26.
26. Tachibana A, Yamaguchi K, Kawauchi S, Kurosaki Y, Yamabe T. Silyl radical mechanisms for silicon-nitrogen bond formation. J Am Chem Soc. 1992;114(19):7504–7.
27. Sun X, Liu HT, Cheng HF. Oxidation behavior of silicon nitride fibers obtained from polycarbosilane fibers via electron beam irradiation curing. RSC Adv. 2017;7(75):47833–9.
28. Shokri B, Firouzjah MA, Hosseini SI. FTIR analysis of silicon dioxide thin film deposited by metal organic-based PECVD, Proceedings of 19th International Symposium on plasma chemistry society. Germany: Bochum; 2009.
29. Liao WS, Lin CH, Lee SC. Oxidation of silicon nitride prepared by plasma-enhanced chemical vapor deposition at low temperature. Appl Phys Lett. 1994;65(17):2229–31.
30. Lee HI, Park JB, Xianyu W, Kim K, Chung JG, Kyoung YK, et al. Degradation by water vapor of hydrogenated amorphous silicon oxynitride films grown at low temperature. Sci Rep. 2017;7(1):14146.

How to cite this article: Kim J, Jeong W, Lee S, Jeong S, Ko Park S-H. Effect of H_2 addition during PECVD on the moisture barrier property and environmental stability of H:SiN_x film. J Am Ceram Soc. 2021;00:1–8. https://doi.org/10.1111/jace.18000